Correlation of the Performance of a PEM Fuel Cell at Different Channel Geometries

I. Khazaee* and M. Ghazikhani

Engineering Faculty, Mechanical Engineering Department, Ferdowsi University of Mashhad, Mashhad, P.O. Box 9177948944-1111, Iran

In this study, the performance of a proton exchange membrane fuel cell at different channel geometries is investigated experimentally. Three PEM fuel cells with different channel geometries with 25 cm^2 active area and Nafion 117 as membrane with 0.004 g/cm^2 platinum for the anode and cathode are employed as a membrane electrode assembly. Some parameters such as input oxygen temperature ($45^\circ C \leq T_{O_2} \leq 65^\circ C$), input hydrogen temperature ($40^\circ C \leq T_{H_2} \leq 60^\circ C$), cell temperature ($45^\circ C \leq T_{cell} \leq 65^\circ C$), input pressure ($1.905\,bar \leq P \leq 4.905\,bar$), oxygen flow rate ($0.5\,L/min \leq \dot{m}_{O_2} \leq 0.1.3\,L/min$), hydrogen flow rate ($0.3\,L/min \leq \dot{m}_{H_2} \leq 0.9\,L/min$) and geometry of channels ($1 \leq Z \leq 3$) affect the performance of the cell. A series of experiments are carried out to investigate the influence of the above parameters on the polarisation curve under the above conditions. A semi empirical equation is offered to correlate the data for the polarisation curve. The results show that when the geometry of channel is rectangular, the performance of the cell is better than the triangular and elliptical channel. Also, results show that increase in the operating temperature and pressure can enhance the cell performance and they are compared with the results of the correlated equation and a good agreement exists.

Keywords: fuel cell, channel geometry, curve fitting, performance, operating parameters

INTRODUCTION

Proton exchange membrane fuel cells (PEMFCs) represent a viable alternative power source for various applications. However, to satisfy the requirements for compactness, low cost, high power density, performance and stability, various aspects of the PEMFC must be optimised. Among the various fuel cell types, the proton exchange membrane (PEM) fuel cell is drawing more attention due to its low operating temperature, ease of start-up and shut-down and compactness. Furthermore, the PEM fuel cell is being investigated as an alternate power generation system especially for distributed generation and transportation. The PEM fuel cell is providing reliable power at steady state; however, it is not able to respond promptly to a load step change. Since the fuel cell is an electrochemical energy conversion device that converts fuel into electricity, its dynamic behaviour depends both on chemical and thermodynamic processes that described by Larminie and Dicks (2003). The polymer electrolytes work at low temperature, which brings this further advantage that a PEM fuel cell can start quickly. PEM fuel cells are being actively developed for use in cars and buses, as well as for a very wide range of portable applications, and also for combined heat and power systems.

In the present work, the effects of oxygen and hydrogen temperature, cell temperature, input pressure, oxygen and hydrogen flow rate and geometry of channels on the performance of a PEM fuel cell have been studied experimentally. Several polarisation curves have been obtained in different conditions, displaying the trend of the cell voltage against current. The main objective of this paper contrary to another works is to analyse the influence of different geometries of the channels or flow fields on the voltage (and consequently the electric power) supplied to a PEM fuel cell at different levels of cell current. Also for obtained results, a semi empirical equation of polarisation curve for PEM fuel cell is developed that the results of it had good agreement with the experimental results.

*Author to whom correspondence may be addressed.
E-mail address: imankhazaee@yahoo.com
Can. J. Chem. Eng. 9999:1–7, 2011

DOI 10.1002/cjce.21632
Published online in Wiley Online Library (wileyonlinelibrary.com).

PREVIOUS WORKS

Scrivano et al. (2009) presented an experimental analysis of a 6 W PEMFC system, including on-site hydrogen production by electrolysis. They investigated the effects of environmental parameters such as the external temperature and the humidity of the gases on the performance of fuel cells. Also they proposed a simple semi-empirical mathematical model capable to perform rough prediction on the behaviour of such systems when exposed at different ambient temperatures that this model threats the stacks of fuel cell, not investigating singularly the inner phenomena which occur in the cell.

Amphlett et al. (1995a, b) investigated a theoretical model, which was employed to provide the structure of the equations, and then, the parameters of these equations were found by using the regression techniques to fit the experimental results. Also they studied a semi-empirical model with a theoretical background that takes into account the main variables of the fuel cell operation such as the operating temperature, the partial pressures at the electrodes and the fuel cell current.

Del Real et al. (2007) investigated a simple empirical equation to model the fuel cell voltage with considering the variations of the main process variables. The model equation has 11 parameters: one parameter related to the mass of liquid water at the anode channel must be estimated due to technical constraints, and the other parameters are obtained from experimental data. Although the model proposed by them, fitted well with the experimental data, the equation of the fuel cell voltage does not have a theoretical basis, and, therefore, it is based on assumptions relating to the effects of temperature and partial pressures that are not proven to be general for fuel cells other than those used by Del Real et al. (2007).

Berning and Djilali (2005) using a three-dimensional computational model for a single cell with an active area of 25 cm^2 and single-serpentine flow field, investigated the influence of this parameter on the cell performance.

Yi and Nguyen (1999), used the numerical methods to solve a two-dimensional single-phase PEMFC model with interdigitated flow channels so as to evaluate the effects of inlet and exit pressures, gas diffusion layer thickness and carbon plate width on the performance of PEMFC.

Cownden et al. (2001) gave a novel study on the performance analysis of a PEM fuel cell system including the system components other than the fuel cell stack, such as compressor, hydrogen supply and the cooling system. Based on the first and second laws of thermodynamics, they suggested that substantial improvements could be made in the performance of the fuel cell system.

Xue and Dong (1998) used a semi-empirical model of the Ballard Mark IV fuel cell and models for the auxiliary systems to create a model of the fuel cell system. Using this model and numerical optimisation, the optimal active stack area and air stoichiometric ratio was obtained to maximise net power output, and, at the same time, minimised production costs.

Ferng et al. (2004) performed analytical and experimental work to investigate a single PEM fuel cell. In their paper, they presented a study of the cell performance covering the effects of operating temperature and pressure on performance and the flow characteristics within the cell. Their paper shows the positive effects of temperature and pressure on the performance of a single PEM fuel cell.

DESCRIPTION OF THE EXPERIMENTS AND METHOD OF THE MEASUREMENTS

A set-up has been constructed for experimental investigation of the performance of the fuel cell. A schematic flow of the test bench is shown in Figure 1. It allows controlling several physical parameters, and the measurement of many output data.

The test bench is made up of four main subsystems. First, the gases supply system, which sends the oxygen and hydrogen flow into the system. Second, the two humidifiers that humidify the oxygen and hydrogen before going into the cell. Third, the nitrogen supply system is applied to inert any flammable mix inside the ducts and to purge the system before activation. Finally, the electrical power supply, regulated from an AC/DC voltage regulator driven from the control panel. The examined prototype can operate at a maximum 5 bar absolute pressure; a pressure regulator valve is included, to make possible to vary the operating pressure of the FC system and the accuracy of monitoring the pressure is $\pm 2\%$. Two flow meters are used to measure the flow rate of the oxygen and hydrogen that the accuracy of them is ± 0.1 L/min.

In order to plot the polarisation curve (I–V curve), we must use the electrical power that produced by the fuel cell by a user and by changing the current and voltage with changing the electrical resistance of the user plot the polarisation curve. For this reason a resistors box was used to change the resistance of the user of electric power that the accuracy of monitoring the voltage and current is $\pm 1\%$. The resistors box, located outside the test chamber, is manually operated; the box and the cables do not introduce

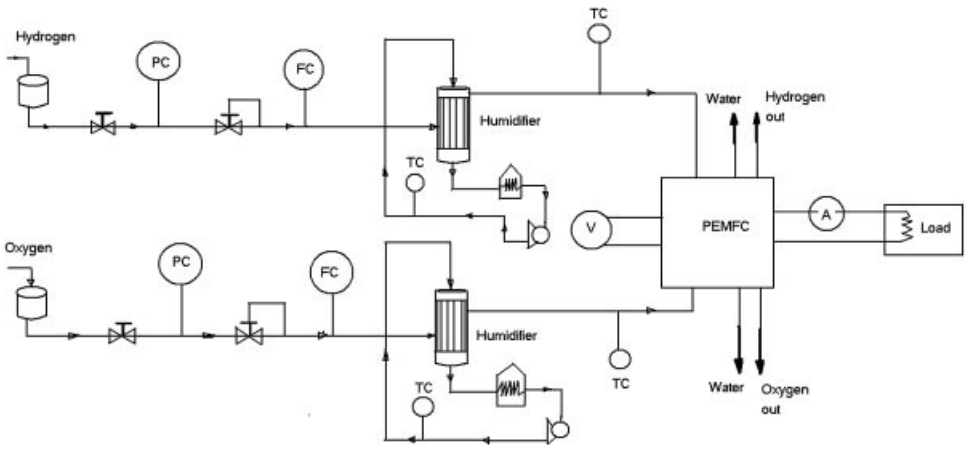

Figure 1. Schematic of the PEMFC system.

relevant errors because they are shielded from external magnetic fields (due to the very low current values). In order to operate in equilibrium conditions, current and voltage values corresponding to each particular value of the total resistance were measured after a sufficient time period to ensure stationary conditions to have been reached as concerns both fuel cell performance and the values of humidity and temperature in the test chamber. The temperature of the inlet gases was measured by digital thermometer with $\pm 0.1^{\circ}$C accuracy.

The specifications of the test system for this study are:

- The humidifier system is membranous.
- The test bench has the system of announcement the leakage of hydrogen.
- The system can control and show the temperature of the oxygen and hydrogen.
- The system can control and show the temperature of the cell.
- The system can control and show the flow rate of the oxygen and hydrogen.
- The system can control and show the inlet pressure of the oxygen and hydrogen.
- The system can show the voltage of the cell.
- The system can show the current of the cell.

Table 1 shows the limits of operating parameters of the experimental setup in this study. The PEM fuel cells considered in this study are a single cell with the size of $45 \times 95 \times 101\,\text{mm}^2$ and an active area of $25\,\text{cm}^2$ and serpentine flow field geometries of channels with the weight of 1300 g. The width, land width and depth of the channel were selected to be 1, 0.8 and 1.27 mm for elliptical channel and 1, 0.8 and 1 mm for rectangular channel and 1, 0.8 and 2 mm for triangular channel, respectively. For a bipolar plate, non-porous graphite is selected. A Nafion 117 membrane with $0.004\,\text{g/cm}^2$ platinum for the anode and cathode was employed as a membrane electrode assembly. On both sides of the MEA, there were 0.33 mm thick carbon papers that acted as diffusion layers. The thickness of the catalyst layer and the PEM is about 0.01 mm and 0.051 mm. The geometry of the channels of the cell in the experimental set-up is shown in Figure 2.

The changed parameters are: input oxygen temperature (T_{O_2}), input hydrogen temperature (T_{H_2}), cell temperature (T_{cell}), input pressure (P), oxygen flow rate ($\dot{m}_{O_2}$) and hydrogen flow rate ($\dot{m}_{H_2}$) and the measured parameters are voltage and current of the cell.

For measuring the inlet temperature of oxygen and hydrogen two digital thermometers are used and the locations of these thermometers are at the inlet tubes. But for measuring the temperature of the cell a different digital thermometer is used that the location of it is at the bipolar plates of the cell. For measuring the flow rate of oxygen and hydrogen two flow meters are used that they measure the flow rate of gases before entering the fuel cell.

At first, all the measurement systems were calibrated and we perform the experiments by humidifying the membrane of the fuel cell by humidifying the gases with saturation water vapour

Table 1. Operational characteristics of the test bench

Voltage	0–2 V
Current	0–20 A
Power	0–22 W
Moisture	100%
Flow rate	0–2 L/min
Gas temperature	Upto 75°C
Cell temperature	Upto 75°C

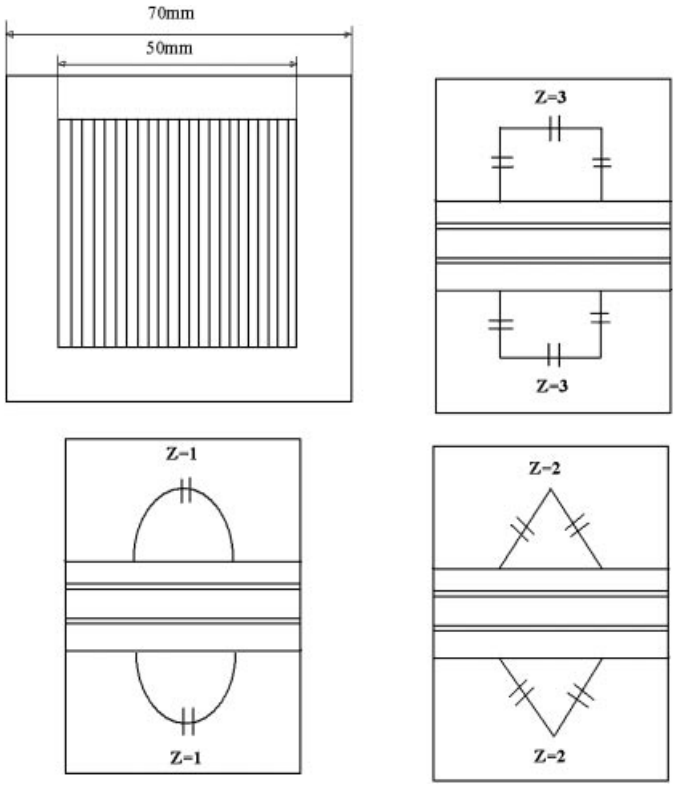

Figure 2. Schematic of the channels PEMFC.

and then change the input oxygen temperature, input hydrogen temperature, cell temperature, input pressure, oxygen flow rate and hydrogen flow rate and measure the pointed parameters and the voltage and the current of the cell after steady state condition. Figure 3 shows a photo of experimental set-up. In this figure, the components of testing a fuel cell such as the PEM fuel cell, temperature indicators, flow meters, the oxygen and hydrogen tank, the humidifier of the gases and the switch keys are shown.

RESULTS AND DISCUSSION

The main goal of this study is to investigate the effects of important parameters and channel geometry on the performance and polarisation curve of a PEM fuel cell. The Range of changing the

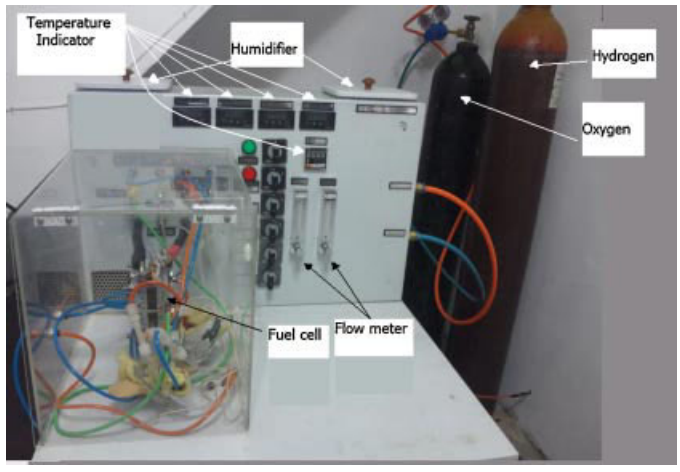

Figure 3. A photo of the experimental set-up.

Table 2. Range of changing the parameters in this study

Description	Unit	Value
Oxygen flow rate	L/min	0.5–1.3
Hydrogen flow rate	L/min	0.3–1.1
Anode inlet pressure	Bar	1–4
Cathode inlet pressure	Bar	1–4
Cell temperature	°C	40–60
Oxygen temperature	°C	45–65
Hydrogen temperature	°C	40–60

parameters in this study is shown in Table 2 and the experiments for each of the parameters done and repeated while the steady state condition occurred.

In Figure 4, the effect of channel geometry on the overall cell performance of three PEM fuel cells for $T_{cell} = 60°C$, $T_{O_2} = 55°C$, $T_{H_2} = 55°C$, $\dot{m}_{O_2} = 0.5$ L/min, $\dot{m}_{H_2} = 0.3$ L/min and $P = 2.905$ bar is shown. It is clear that when the geometry of the cell is rectangular, the overall cell performance is better than the elliptical geometry and triangular geometry that this is due to decrease in penetration of the gases into the gas diffusion layer and decreasing the chemical reaction at the surface of catalyst layers.

Figure 5 illustrates the polarisation curves of the PEM fuel cell to investigate the influence of the input pressure gases on the overall fuel cell performance at $T_{cell} = 60°C$, $T_{O_2} = 55°C$, $T_{H_2} = 55°C$, $\dot{m}_{O_2} = 0.5$ L/min and $\dot{m}_{H_2} = 0.3$ L/min. It is clear that an increase in pressure increases the performance of the fuel cell which is due to decrease of ohmic and concentration losses and increase more efficient fuel transport from the gas diffusion layers and the chemical reaction at the catalyst surfaces and exchange current density.

As can be seen, higher cell-operating pressure results in more even distribution of the local current density due to the high oxygen concentration at the catalyst layer. This leads to the fact that for a lower cell-operating pressure at a constant nominal current density, there is a much stronger distribution of current inside the cell, the maximum local current density being at the inlet under the channel area.

In Figures 6 and 7, the effect of hydrogen flow rate and oxygen flow rate of the anode and cathode sides at the overall cell performance of the PEM fuel cell for $T_{cell} = 60°C$, $T_{O_2} = 55°C$, $T_{H_2} = 55°C$, $\dot{m}_{O_2} = 0.5$ L/min and $P = 2.905$ bar are shown. It is clear that by increasing the hydrogen flow rate from 0.3 L/min to 0.7 L/min and the oxygen flow rate from 0.5 L/min to 0.9 L/min the cell performance enhances but when the flow rate increases from 0.7 L/min to 0.9 L/min for hydrogen and from 0.9 L/min to 1.3 L/min the cell performance decreases. It is due to that by increasing the flow rate of hydrogen and oxygen more fuel and oxidiser transport from GDL to the catalyst layer and the electrochemical reaction enhances but when the flow rate of hydrogen and oxygen increase from 0.7 L/min and 0.9 L/min the transportation of fuel and oxidiser to the GDL decrease and they come out from the channel without an electrochemical reaction. Also, it is clear that when $i \leq 0.1$ A/cm^2 for hydrogen and $i \leq 0.05$ A/cm^2 for oxygen the performance of the cell is better when the flow rate decreases.

Figure 8 shows the effect of cell temperature on the performance of the cell at $P = 2.905$ bar, $T_{O_2} = 55°C$, $T_{H_2} = 55°C$, $\dot{m}_{O_2} = 0.5$ L/min and $\dot{m}_{H_2} = 0.3$ L/min. It is clear that increasing in the cell temperature leads to the increase in the performance of the cell which is due to the decreasing of activation overpotential

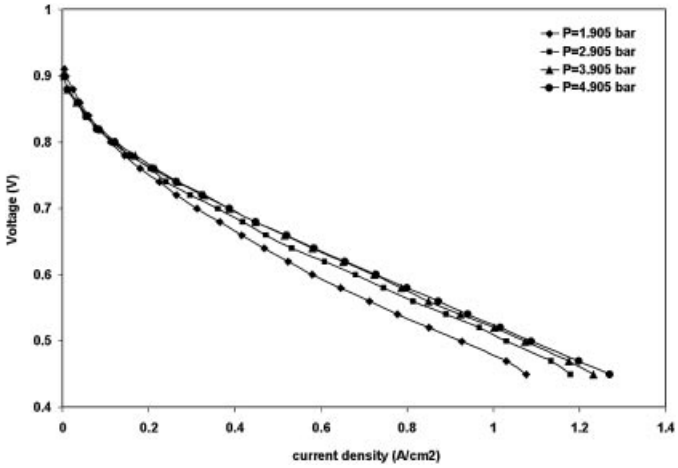

Figure 5. Variation of cell performance at different cell pressures for $T_{cell} = 60°C$, $\dot{m}_{O_2} = 0.5$ L/min, $\dot{m}_{H_2} = 0.3$ L/min, $T_{O_2} = 55°C$ and $T_{H_2} = 55°C$.

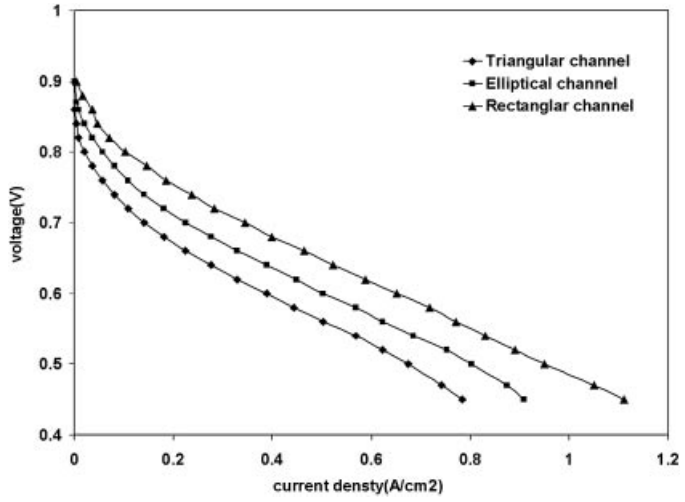

Figure 4. Variation of cell performance at different channel geometry for $T_{cell} = 60°C$, $\dot{m}_{O_2} = 0.5$ L/min, $\dot{m}_{H_2} = 0.3$ L/min, $P = 2.905$ bar, $T_{O_2} = 55°C$ and $T_{H_2} = 55°C$.

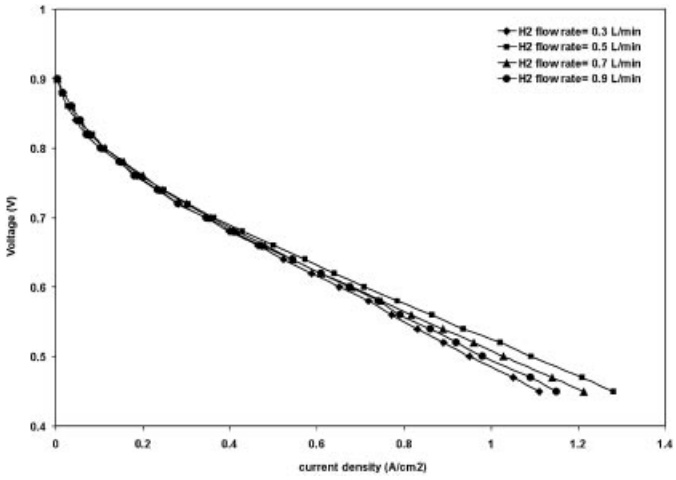

Figure 6. Variation of cell performance at different hydrogen flow rates for $T_{cell} = 60°C$, $\dot{m}_{O_2} = 0.5$ L/min, $P = 2.905$ bar, $T_{O_2} = 55°C$ and $T_{H_2} = 55°C$.

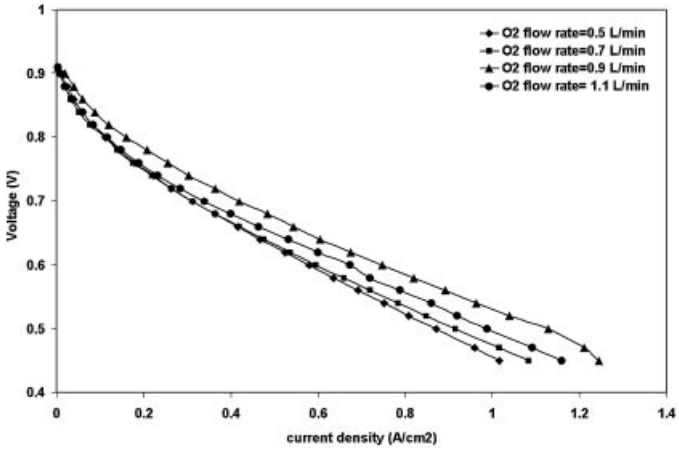

Figure 7. Variation of cell performance at different oxygen flow rates for $T_{cell} = 60^{\circ}C$, $\dot{m}_{H_2} = 0.3$ L/min, $P = 2.905$ bar, $T_{O_2} = 55^{\circ}C$ and $T_{H_2} = 55^{\circ}C$.

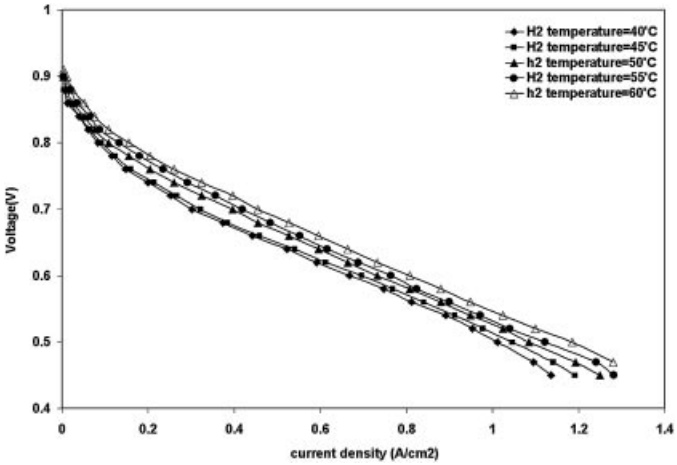

Figure 9. Variation of cell performance at different hydrogen temperatures for $P = 2.905$ bar, $\dot{m}_{H_2} = 0.3$ L/min, $\dot{m}_{O_2} = 0.5$ L/min, $T_{O_2} = 55^{\circ}C$ and $T_{cell} = 60^{\circ}C$.

and increase in the electrochemical reaction. This is because of the exchange current density of the oxygen reduction reaction, which increases rapidly with temperature due to the enhanced reaction kinetics, which reduces activation losses. A higher temperature leads also to a higher diffusivity of the hydrogen protons in the electrolyte membrane, thereby reducing the membrane resistance and this leads to reducing the potential loss in the membrane. Also Figure 8 indicates that at the conditions of the higher operating voltage (lower over-potential), the influence of the internal flow modification on the overall fuel cell performance is negligibly small. At lower operating voltage conditions, on the other hand, the effect of the internal flow modification on the polarisation curves becomes important.

The temperature basically affects all the different transport phenomena inside the fuel cell. The composition of the incoming gas streams depends strongly on the temperature. Assuming the inlet gases are fully humidified, the partial pressure of water vapour entering the cell depends on the temperature only. Thus, the molar fraction of water vapour is a function of the total inlet pressure and temperature, and so the molar fraction of the incoming hydrogen and oxygen depend on the temperature and pressure as well. In Figures 9 and 10, the effect of input hydrogen temperature and input oxygen temperature of the anode and cathode sides at the overall cell performance of the PEM fuel cell for $T_{cell} = 60^{\circ}C$, $\dot{m}_{H_2} = 0.3$ L/min, $\dot{m}_{O_2} = 0.5$ L/min and $P = 2.905$ bar are shown. It is clear that at the conditions of the higher operating voltage (lower over-potential), the influence of the oxygen temperature on the overall fuel cell performance is negligibly small but at lower operating voltage conditions the effect of input temperature on the polarisation curves becomes important. Also, it is clear that by increasing the hydrogen and oxygen temperatures the cell performance enhances that it is due to the decreasing of activation overpotential and increase in the electrochemical reaction at the catalyst surfaces.

A New Correlation for Polarisation Curve

By doing the experiments, it is clear that some parameters such as input oxygen temperature (T_{O_2}), input hydrogen temperature (T_{H_2}), cell temperature (T_{cell}), input pressure (P), oxygen flow rate ($\dot{m}_{O_2}$), hydrogen flow rate ($\dot{m}_{H_2}$) and channel geometry

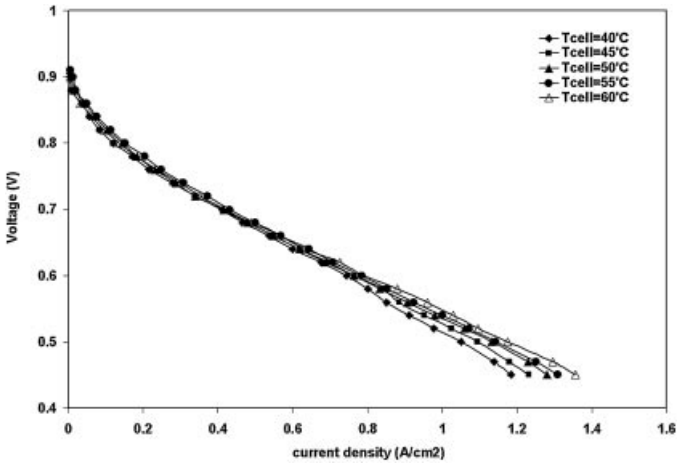

Figure 8. Variation of cell performance at different cell temperatures for $P = 2.905$ bar, $\dot{m}_{H_2} = 0.3$ L/min, $\dot{m}_{O_2} = 0.5$ L/min, $T_{O_2} = 55^{\circ}C$ and $T_{H_2} = 55^{\circ}C$.

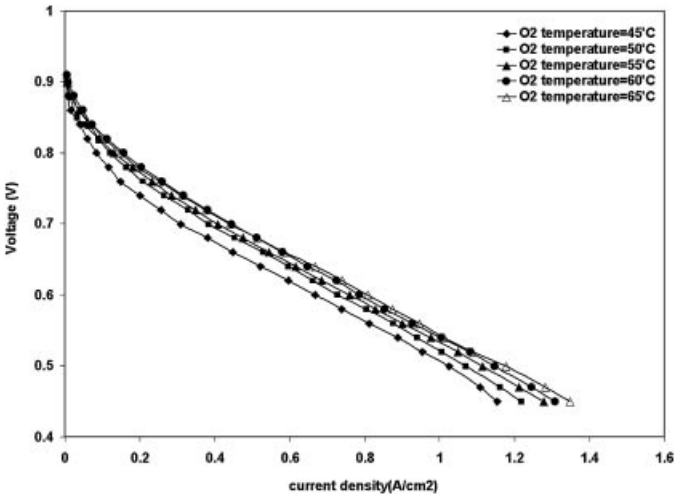

Figure 10. Variation of cell performance at different oxygen temperatures for $P = 2.905$ bar, $\dot{m}_{H_2} = 0.3$ L/min, $\dot{m}_{O_2} = 0.5$ L/min, $T_{H_2} = 55^{\circ}C$ and $T_{cell} = 60^{\circ}C$.

specification (Z) affect the performance of the cell. The main reason of changing the performance by changing these parameters is the electrochemical reaction at the catalyst surfaces but the more details described in previous sections. The method of fitting used in this paper is the least square method. This method fits a set of data points (x_i, y_i) to a function that is a combination of any number of functions of the independent variable x. The goal of nonlinear regression is to determine the best-fit parameters for a model by minimising a chosen merit function. Where nonlinear regression differs is that the model has a nonlinear dependence on the unknown parameters, and the process of merit function minimisation is an iterative approach. The process is to start with some initial estimates and incorporates algorithms to improve the estimates iteratively. The new estimates then become a starting point for the next iteration. These iterations continue until the merit function effectively stops decreasing. The nonlinear model to be fitted can be represented by:

$$y = y(x; a) \tag{1}$$

The merit function minimised in performing nonlinear regression the following:

$$\chi^2(a) = \sum_{i=1}^{N} \left\{ \frac{y_i - y(x_i; a)}{\sigma_i} \right\}^2 \tag{2}$$

Where σ_i is the measurement error, or standard deviation of the ith data point. For understanding how the results calculated we have:

The ith predicted, or fitted value of the dependent variable Y, is denoted by $\hat{Y}_i$. This value is obtained by evaluating the regression model $\hat{Y} = f(X, \hat{\beta}_j)$, where $\hat{\beta}_j$ are the regression parameters, or variables. Then the residuals $(Y_i - \hat{Y}_i)$ and sum of the residuals $\sum_{i=1}^{n} (Y_i - \hat{Y}_i)$ calculated and then, the average of residuals and residual of sum of squares calculated.

SSE = Residual or Error Sum of Squares (Absolute) = $\sum_{i=1}^{n} (Y_i - \hat{Y}_i)^2$; SSE_R = Residual or Error Sum of Squares (Relative) = $\sum_{i=1}^{n} [(Y_i - \hat{Y}_i)^2 * W_i]$where $W_i = 1/\sigma_i^2$ normalised so that $\sum_{i=1}^{n} W_i = n$.

σ_i = the standard deviation of the ith data point Y_i and n is the number of data points, or observations.

The principle behind nonlinear regression is to minimise the residual sum of squares by adjusting the parameters $\hat{\beta}_j$ in the regression model to bring the curve close to the data points. This parameter is also referred to as the error sum of squares, or *SSE*. If the residual sum of squares is equal to 0.0, the curve passes through every data point.

Thus, the correlation that proposed to indicate the effect of those parameters on the polarisation curve is:

$$V = a + bi^k + ciZ^n \left(\frac{T_{\text{H}_2}}{T_{\text{cell}}}\right)^d \left(\frac{T_{\text{O}_2}}{T_{\text{cell}}}\right)^e \left(\frac{\dot{m}_{\text{O}_2}}{\dot{m}_{\text{H}_2}}\right)^f P^g + lZ^h[\exp(m + pi)]^j \tag{3}$$

that in this equation current density is in A/cm^2, temperatures are in °C, flow rates are in L/min, ambient pressure is in bar and $Z = 1$ for elliptical channel and $Z = 2$ for triangular channel and $Z = 3$ for rectangular channel.

Table 3. Value and limits of constants in Equation (3)

Variable	Value	Lower limit	Upper limit
a	0.872654001	0.868892869	0.876415133
b	−0.191011137	−0.199909826	−0.182112449
c	−0.27134189	−0.284603833	−0.258079947
d	−9.9E−02	−0.13058875	−6.87E−02
e	−0.1375614	−0.173141973	−0.101980826
f	−2.69E−02	−3.41E−02	−1.97E−02
g	−0.132698922	−0.153154262	−0.112243582
h	13.85642525	−3.472674784	31.18552528
m	−6.228078322	−124161.6701	124149.2139
j	1.775427703	−59501.80159	59505.35244
k	0.368901517	0.33917133	0.398631704
l	7.89E−04	−137.8906155	137.8921933
n	0.216711724	0.195475458	0.23794799
p	0.548819575	−18393.17559	18394.27323

In Equation (3), the constants a, b, c, d, e, f, g, h, j, k, l, m and n are undefined and by using software as Datafit which fits the results of experiment from one to more independent variables that in Table 3 the value, upper limit and lower limit of constants in Equation (3) was shown. Hence, by analysing the results of experiments, Equation (3) converts into Equation (4) as:

$$V = 0.8726 - 0.191i^{0.369} + 7.888 \times 10^{-4} Z^{13.86} \exp(-11.055 + 0.974i) - \frac{0.2713iZ^{0.2167}}{p^{0.1327}\left(\frac{T_{\text{H}_2}}{T_{\text{cell}}}\right)^{0.0996}\left(\frac{T_{\text{O}_2}}{T_{\text{cell}}}\right)^{0.1375}\left(\frac{\dot{m}_{\text{O}_2}}{\dot{m}_{\text{H}_2}}\right)^{0.0269}} \tag{4}$$

Figure 11 shows the comparison between the experimental results and the correlated equation of the polarisation curve for $T_{\text{O}_2} = 55°\text{C}$, $T_{\text{H}_2} = 55°\text{C}$, $T_{\text{cell}} = 60°\text{C}$, $P = 3.905$ bar, $\dot{m}_{\text{O}_2} = 0.5$ L/min, $\dot{m}_{\text{H}_2} = 0.3$ L/min and three different channel geometries. It is clear that there are significant agreements with them.

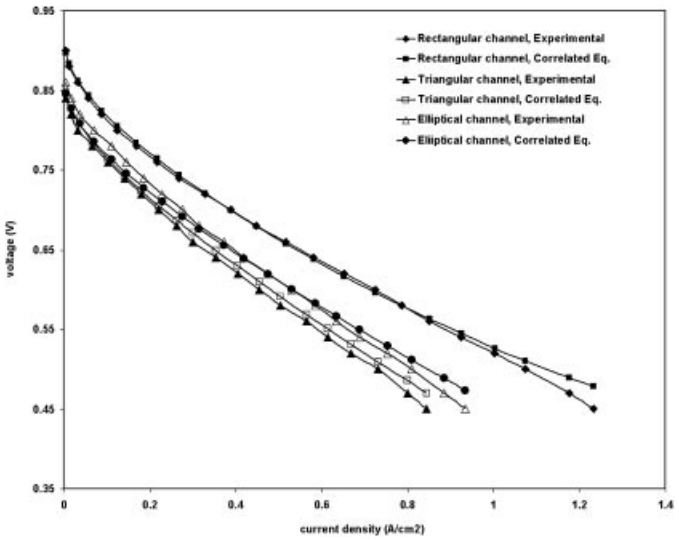

Figure 11. Comparison between experimental results and results of correlated equation for $P = 3.905$ bar.

CONCLUSION

In this study, the effects of input oxygen temperature (T_{O_2}), input hydrogen temperature (T_{H_2}), cell temperature (T_{cell}), input pressure (P), oxygen flow rate ($\dot{m}_{O_2}$), hydrogen flow rate ($\dot{m}_{H_2}$) and channel geometry specification (Z) on the performance and polarisation curve of a PEM fuel cell have been investigated. We have found out that:

- When the geometry of the cell is rectangular, the overall cell performance is better than the elliptical geometry and triangular geometry that this is due to decrease in penetration of the gases into the gas diffusion layer and decreasing the chemical reaction at the surface of catalyst layers.
- By increasing the oxygen flow rate the cell performance enhances but when the flow rate increases from 0.9 L/min to 1.3 L/min the cell performance decreases.
- Increasing in the cell temperature leads to the increase in the performance of the cell, which is due to the decreasing of activation overpotential and increase in the electrochemical reaction.
- The effect of oxygen and hydrogen temperature on the performance of the cell is so important that by increasing the hydrogen and oxygen temperatures the cell performance enhances that it is due to the decreasing of activation overpotential and increase in the electrochemical reaction.
- A new correlation for predicting the polarisation curve of a PEM fuel cell according to input oxygen temperature, input hydrogen temperature, cell temperature, input pressure, oxygen flow rate, hydrogen flow rate and channel geometry was proposed and there was a good agreement between its results and the experimental results.

ACKNOWLEDGEMENTS

This work was partially supported by Renewable Energy Organisation of Iran.

REFERENCES

Amphlett, J. C., R. M. Baumert, R. F. Mann, B. A. Peppley and P. R. Roberge, "Performance Modelling of the Ballard Mark IV Solid Polymer Electrolyte Fuel Cell. I-Mechanistic Model Development," Electrochem. Sci. Technol. **142**, 1–8 (1995a).

Amphlett, J. C., R. M. Baumert, R. F. Mann, B. A. Peppley and P. R. Roberge, "Performance Modelling of the Ballard Mark IV Solid Polymer Electrolyte Fuel Cell. II-Empirical model development," Electrochem. Sci. Technol. **142**, 9–15 (1995b).

Berning, T. and N. Djilali, "Three-Dimensional Computational Analysis of Transport Phenomena in a PEM fuel cell – A Parametric Study," J. Power Sources **124**, 440–452 (2005).

Cownden, R., M. Nahon and M. A. Rosen, "Modelling and Analysis of a Solid Polymer Fuel Cell System for Transportation Applications," Int. J. Hydrogen Energ. **26**, 615–623 (2001).

Del Real, A. J., A. Arce and C. Bordons, "Development and Experimental Validation of a PEM Fuel Cell Dynamic Model," J. Power Sources **173**, 310–324 (2007).

Ferng, Y. M., Y. C. Tzang, B. S. Pei, C. C. Sun and A. Su, "Analytical and Experimental Investigations of a Proton Exchange Membrane Fuel Cell," Int. J. Hydrogen Energ. **29**, 381–391 (2004).

Larminie, J. and A. Dicks, "Fuel Cell System Explained," 2nd ed., Wiley, Chichester, England (2003).

Scrivano, G., A. Piacentino and F. Cardona, "Experimental Characterisation of PEM Fuel Cells by Micro-Models for the Prediction of On-Site Performance," Renew. Energ. **34**, 634–639 (2009).

Xue, D. and Z. Dong, "Optimal Fuel Cell System Design Considering Functional Performance and Production Costs," J. Power Sources **76**(1), 69–80 (1998).

Yi, J. S. and T. V. Nguyen, "Multi Component Transfer in Porous Electrodes of Proton Exchange Membrane Fuel Cells Using the Interdigitated Gas Distributors," J. Electrochem. Soc. **146**, 38–45 (1999).

Manuscript received June 30, 2011; revised manuscript received December 1, 2011; accepted for publication December 8, 2011.